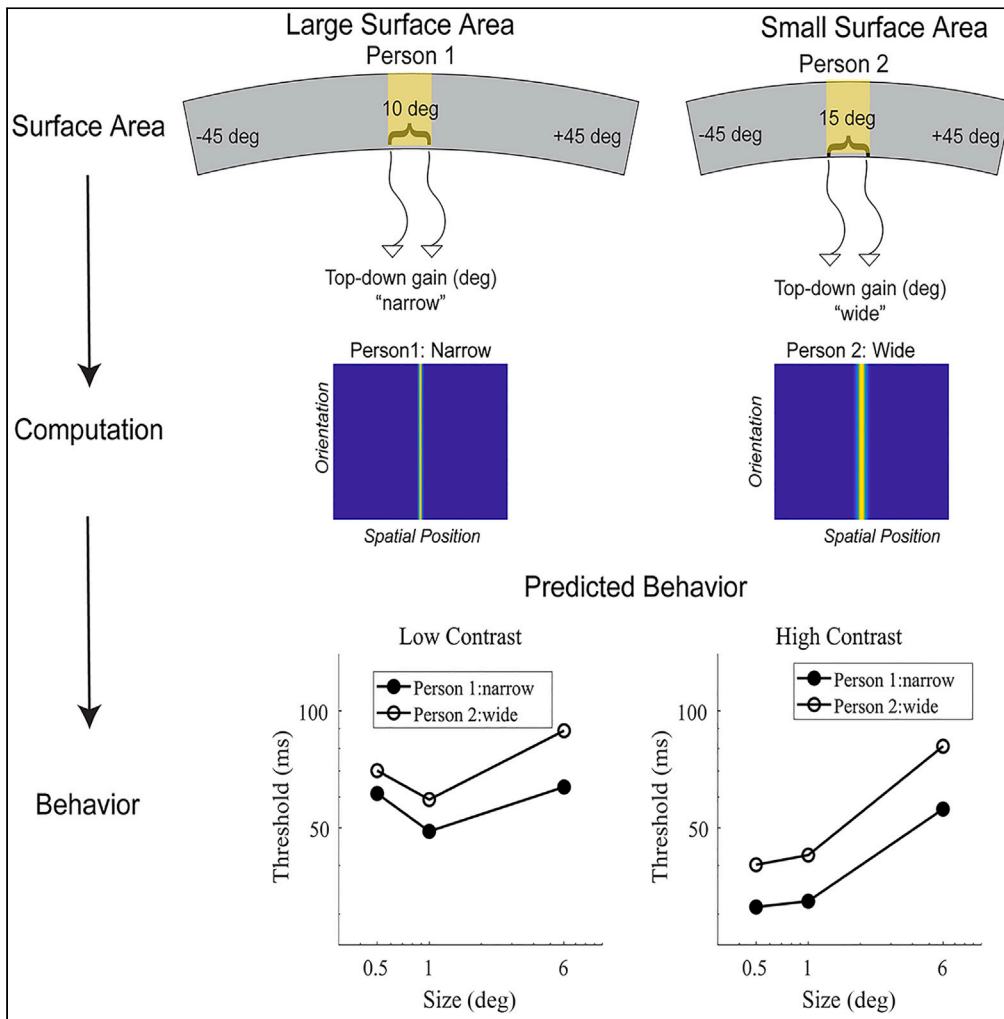**Article**

Linking cortical surface area to computational properties in human visual perception

Scott O. Murray,
Tamar Kolodny,
Sara Jane Webb

somurray@uw.edu

Highlights

Cortical surface area (SA) influences visual perception

Surface area variations link to behavior in motion task

Divisive normalization model explains SA effects

Findings extend to ASD, enhancing model utility

Article

Linking cortical surface area to computational properties in human visual perception

Scott O. Murray,[1,5,*] Tamar Kolodny,[2] and Sara Jane Webb[3,4]

SUMMARY

Cortical structure and function are closely linked, shaping the neural basis of human behavior. This study explores how cortical surface area (SA), a structural feature, influences computational properties in human visual perception. Using a combination of psychophysical, neuroimaging, and computational modeling approaches, we find that variations in SA across the parietal and frontal cortices are linked to distinct behavioral patterns in a motion perception task. These differences in behavior correspond to specific parameters within a divisive normalization model, indicating a unique contribution of SA to the spatial organization of cortical circuitry. This work highlights the importance of cortical architecture in modifying computational processes that underlie perception, enhancing our understanding of how structural differences can influence neural function and behavior.

INTRODUCTION

The surface area (SA) of cortical regions varies widely across individuals, even after adjusting for differences in overall brain size. Proportionally greater SA is observed in some regions compared to other regions, and this variation has been associated with behavior in a wide range of cognitive[1–3] and perceptual[4,5] domains and clinical conditions.[6–12] However, the impact of these regional SA differences on neural computation and behavior is unknown. We hypothesize that the proportional scaling of SA in a region—determined by whether a region constitutes a relatively large or small portion of the cortex within an individual—affects the organization and spatial properties of neural circuits within that region. We focus our investigation on visual motion processing, examining how individual differences in SA may contribute to variations in perceptual behavior across individuals and the computational mechanisms that may give rise to the specific patterns of behavioral differences.

We measured visual motion duration thresholds—the amount of time a visual motion stimulus needs to be presented in order to perceive its direction. Behavior in this task depends on stimulus size and luminance contrast; paradoxically, larger, high-contrast stimuli require longer presentation durations, reflecting visual surround suppression.[13] We have previously demonstrated that the contrast and size dependency of this perceptual behavior is well accounted for by a divisive normalization model.[14] Divisive normalization describes neural responses in terms of an excitatory drive term, divided by the sum of a spatially broader suppressive drive term, plus a small number, sigma, which controls response sensitivity. Importantly, extensions of this model that include a top-down gain term,[15] reflecting the attentional field, have been used previously to describe responses in a wide range of perceptual and cognitive functions.[16] We speculate that individual differences in performance might be at least partially driven by intrinsic differences in the width of top-down gain. In the current study, we explored the potential origin of individual differences in top-down gain as stemming from cortical SA differences in attentional control regions, with a particular emphasis on parietal and frontal regions.

The rationale behind predicting a relationship between SA and the width of top-down gain is based on the spatial organization of attentional control regions (illustrated in Figure 1). Imagine two individuals with the same total cortical SA, but person 1 has a proportionally larger attentional control region compared to person 2. Attentional control regions are known to be spatiotopically organized.[17–20] Assuming that both individuals have identical spatial properties in their feedback circuitry anatomy, we would expect feedback circuits to represent a spatially narrower region of space in person 1 than in person 2. This is because an equivalent amount of cortex represents a narrower region of space in person 1 than in person 2, leading to a spatially narrower gain amplification in person 1. To fully explore the implications of this spatial difference in top-down gain, we incorporate it into the normalization model (Figure 1B) and make behavioral predictions for these two hypothetical individuals (Figure 1C). In experiment 1, we first test the general hypothesis described by the model predictions in Figure 1C—individuals with proportionally larger attentional control regions will demonstrate shorter motion duration thresholds compared to those with smaller attentional control regions. Then, subsequently, we analyze whether SA is associated with specific parameters of the normalization model such as attention width.

[1]Department of Psychology, University of Washington, Seattle, WA 98195, USA
[2]Department of Psychology and the School of Brain Sciences and Cognition, Ben-Gurion University, Beer Sheva, Israel
[3]Department of Psychiatry and Behavioral Science, University of Washington, Seattle, WA 98195, USA
[4]Seattle Children's Research Institute, 1920 Terry Avenue, Building Cure-03, Seattle, WA 98101, USA
[5]Lead contact
*Correspondence: somurray@uw.edu
https://doi.org/10.1016/j.isci.2024.110490
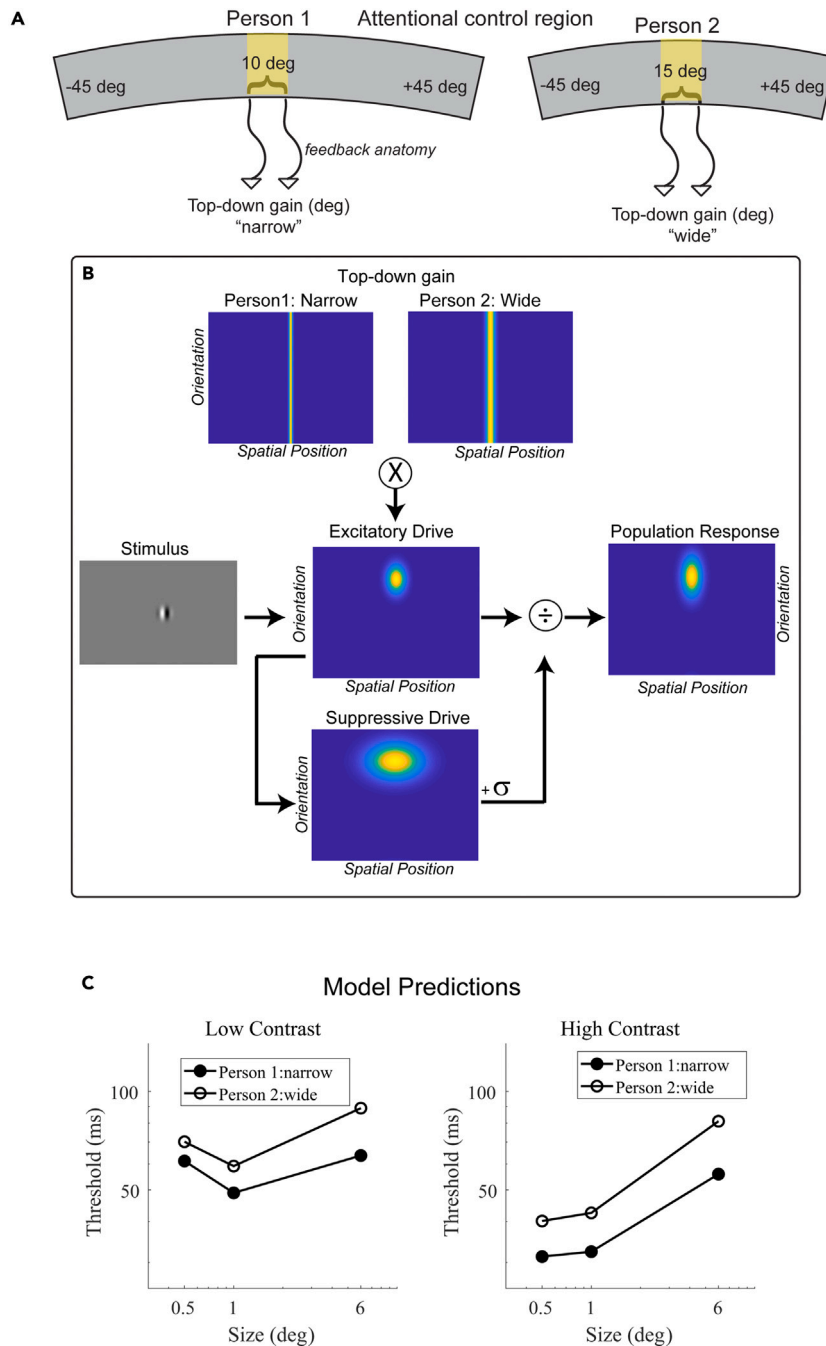
Figure 1. Hypothesized relationship between surface area and its computational and behavioral effects

(A) Schematic illustrating surface area differences between two individuals in a spatiotopically organized attentional control region. An equivalent amount of cortex represents a narrower region of space in person 1 vs. person 2.

(B) Narrow vs. wide top-down gain incorporated into the normalization model.

(C) Predicted duration thresholds from the model for narrow vs. wide top-down gain. Predicted thresholds are derived from the peak population response in the model, assuming higher responses result in shorter thresholds (see STAR Methods).

RESULTS

Experiment 1: Identifying regions where SA is correlated with duration thresholds

We measured motion duration thresholds using three sizes (stimulus radius = 0.5, 1.0, and 6 degrees) and two luminance contrasts (low = 3% and high = 98%), as in previous publications[14,21–23] (Figure 2). See Table 1 for sample sizes and participant demographic information. To test
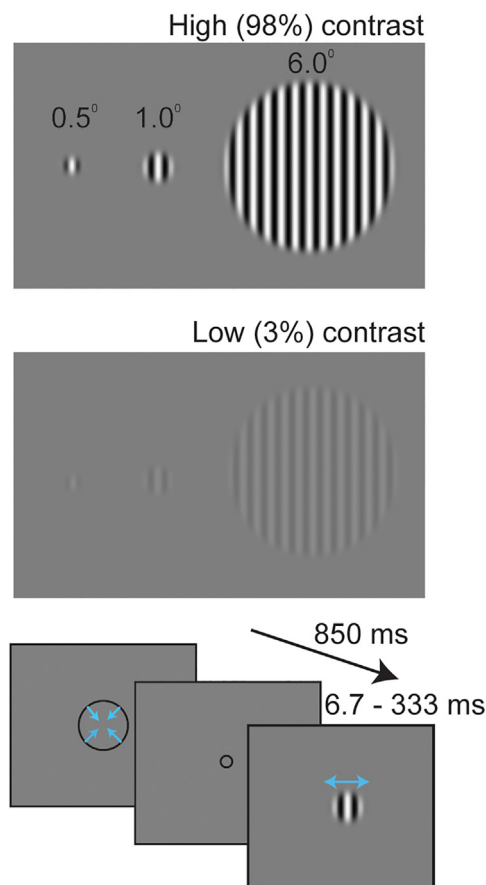
Figure 2. Experimental design

Three different sizes and two luminance contrasts were used. Each trial started with a contracting fixation circle, then a drifting grating was presented and participants indicated whether the motion direction was left or right. Stimuli were presented using an adaptive staircase that adaptively adjusted presentation times to estimate the minimum duration required to perceive leftward or rightward motion ("duration threshold").

the predicted relationship between SA and threshold, we examined the correlation between individual differences in duration threshold and normalized regional SA (results for non-normalized SA are presented in Data S1), as defined using the Human Connectome Project Multimodal Parcellation atlas (HCP-MMP),[24] across 62 individuals. The HCP-MMP is comprised of 180 regions per hemisphere that are defined using cortical thickness, myelin content, functional connectivity, and task-based fMRI (alternative parcellation schemes are compared in Data S2 and S3). At high contrast, there is little difference in duration thresholds for small stimulus sizes.[14,21–23] Thus, to minimize the effects of surround suppression and obtain the most accurate measure of motion duration threshold, we initially focused on behavioral data by averaging thresholds in the two smallest (0.5 and 1.0 degrees) high-contrast conditions (later analyses consider all stimulus conditions).

In line with our prediction, significant negative correlations between thresholds and regional SA were observed within well-known attentional control regions (Figure 3A). Using a statistical threshold of $p < 0.01$ (uncorrected), individual differences in duration thresholds were found to be negatively correlated with individual differences in normalized SA in six parcels of the HCP-MMP atlas—a group of five regions in the right parietal cortex (7AL, VIP, LIPd, IP1, and IP2) and a frontal region in the left hemisphere (11l). Subsequent analyses focus on these "parietal" and "frontal" regions. Relaxing the correlation threshold, for example reducing it to $p < 0.05$, did not substantively alter the regions that correlated with duration thresholds and mostly served to expand the number of identified parietal regions (Figure 3A, lighter shading). The additional regions in the left anterior temporal pole are discussed in Data S4.

While, by definition, the variation in normalized SA in the parietal (summed across the five parcellations) and frontal regions are each significantly negatively correlated with variation in motion duration thresholds (Figure 3B, $r_{55} = -0.47$, $p < 10^{-3}$ and 3C, $r_{55} = -0.40$, $p < 0.01$), the variation in SA between the two regions is uncorrelated (Figure 3D, $r_{60} = 0.15$, $p = 0.25$)—a large or small parietal region in an individual is not related to a large or small frontal region. This suggests that SA differences in the parietal and frontal regions may independently contribute to behavior. To explore this possibility, we separately assessed the relationship between normalized SA and behavior for the parietal and frontal regions. First, for a qualitative assessment of the relationship, we divided participants into two groups based on their summed surface area in the parietal parcels. We then plotted the duration thresholds across all stimulus conditions for the two subject groups (small vs. large parietal

Table 1. Participant demographics

Subject numbers and demographics	N	M/F/NS	Age (mean, SD)
Experiment 1: Psychophysical motion duration threshold task	62	35/27	23.4 (3.4)
Experiment 2: Psychophysical spatial integration task	29	14/13/2	23.1 (3.0)
Experiment 3: ASD cohort	20	12/8	22.5 (3.7)
Experiment 4: FMRI response in hMT+	30	18/12	23.3 (3.5)
Experiment 5: Contrast detection	Same as experiment 1	Same as experiment 1	Same as experiment 1

NS, not specified.

SA; Figure 4A). Recall that for the correlational analysis, aforementioned, we used the average threshold between the high-contrast 0.5- and 1.0-degree conditions; all of the low-contrast conditions and the large, 6.0 degree, condition are used here for the first time. We performed the same group-split analysis based on normalized SA in the frontal cortex (Figure 4B).

To better understand the model predictions and data, particularly the nonmonotonic behavior observed in Figure 4, it is useful to revisit the established patterns typically observed across different stimulus sizes and contrasts.[13,14,21,22] For high-contrast stimuli, an increase in stimulus size paradoxically necessitates a longer presentation duration for accurate discrimination, a phenomenon attributable to enhanced surround suppression. Conversely, for low-contrast stimuli, duration thresholds decrease as the stimulus size increases, conforming to intuitive expectations, until they either plateau or increase at the largest sizes. Adjustments to specific parameters within our normalization model allow us to modify these basic patterns. These modifications enable us to explore how anatomical differences, such as variations in cortical surface area, may influence computational processes underlying these perceptual behaviors.

The group-splits revealed a notably differential association with behavior in the parietal and frontal regions, particularly for low contrast stimuli—a marked difference in behavior for the small but not large stimulus when splitting groups based on parietal SA and a similarly large difference in behavior for the large but not small stimulus when splitting groups based on frontal SA. This differential pattern is further supported by a quantitative analysis–SA in the parietal region correlates with thresholds for the small, low-contrast stimulus ($r_{55} = -0.44$, $p < 0.001$) but not with the large, low-contrast stimulus ($r_{60} = -0.24$, $p = 0.07$) (Figure 5). Conversely, frontal cortex SA exhibits a significant correlation with the large, low-contrast thresholds ($r_{55} = -0.21$, $p = 0.11$) but not with the small, low-contrast thresholds ($r_{60} = -0.29$, $p = 0.02$) (Figure 5).

The observed differences in behavior as a function of SA in the parietal and frontal regions can be explained by distinct parameters of the normalization model. Specifically, the pattern of results in the parietal cortex can be approximated by adjusting the spatial extent of receptive fields of the excitatory drive (Figure 4C)—spatially narrower excitatory drive is predicted to result in lower thresholds for small but not large stimuli (See Data S5 for a range of parameter values and their specific effect on small sizes). This is because the narrower receptive fields result in less engagement of the suppressive surround. When the stimulus is large, small and large spatial receptive fields engage the suppressive surround equally.

The pattern of behavior linked to frontal cortex is distinct from that associated with the parietal cortex and is more closely aligned with our *a priori* hypothesis—it is best accounted for by manipulating the spatial width of top-down gain (Figure 4D). Spatially wide top-down gain more strongly engages the suppressive surround for large compared to small stimuli (See Data S5 for a range of parameter values and their specific effect on large sizes). We found no other model parameters that can produce these unique patterns of results for low contrast stimuli. Overall, these findings suggest that SA in these two regions affects normalization-related circuitry in distinct ways.

Experiment 2: Generalizing the results to a new stimulus configuration

We next aimed to examine the generality of our findings. A subset of the participants took part in a new behavioral experiment, designed to measure individual differences in spatial integration in the motion duration threshold task. The basic configuration of the task is shown in Figure 6. In this task, participants performed the motion duration threshold task using a single, small (0.5 degrees) high-contrast target stimulus. An uninformative high-contrast surrounding stimulus was also presented, which could move in either the same or opposite direction as the central target stimulus. As a result, participants were encouraged to ignore the surround and focus their attention on the central stimulus. The gap between the surround and target varied from 0.5 to 4.5 degrees.

In the context of the current experiment, this stimulus provides an ideal generalization test for the initial findings. First, consider the predictions for behavioral differences based on SA in the parietal cortex. When the surround is moving in the same direction as the target, as the gap between the surround and target becomes very small, the stimulus essentially resembles a single, large high-contrast stimulus. Conversely, when the gap is large, the stimulus appears as a small, isolated high-contrast stimulus. Predictions for these two extreme conditions can be made by revisiting the results of the parietal cortex group split for the high-contrast condition in experiment 1 (Figure 4A). Specifically, in experiment 1, small stimuli were associated with parietal cortex SA variation, while large stimuli were not. This same pattern is observed with small and large gap sizes in experiment 2—when the gap sizes are very small (approximating a large stimulus), there is no association with SA in the parietal cortex; whereas, when gap sizes are large (approximating a small stimulus), an association is present. This
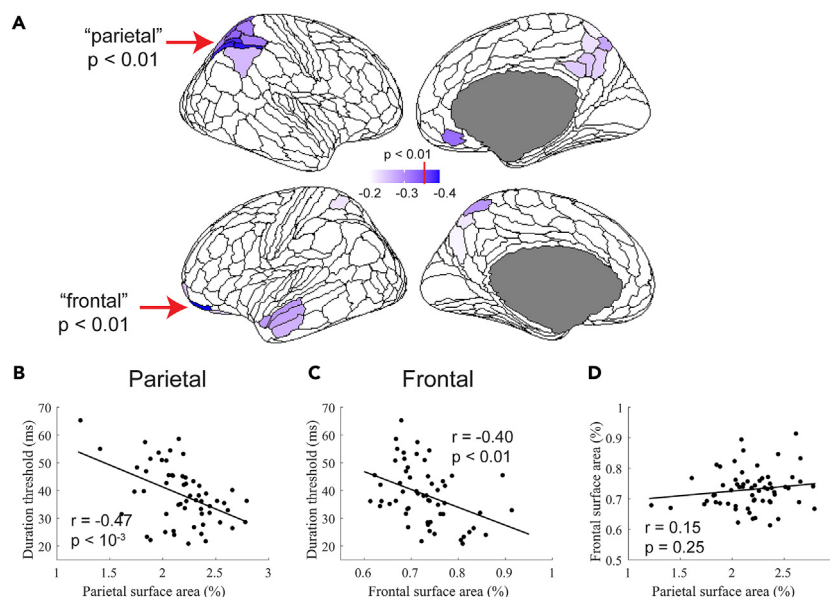
Figure 3. Correlations between surface area and duration thresholds

(A) Regions of the HCP-MMP atlas that negatively correlate with duration threshold. Regions that surpass a $p < 0.01$ are indicated with the red arrows and darker purple color and include 5 parcels in the right parietal cortex and 1 parcel in the left frontal cortex. Significant relationship between individual differences in surface area in the parietal (B) and frontal (C) regions and duration thresholds.

(D) There is no significant relationship between individual differences in surface area between the two regions.

pattern is apparent in both a qualitative analysis based on a group split of parietal cortex SA (Figure 6B) and a quantitative analysis correlating parietal SA variation with duration thresholds across gap sizes (Figure 6D). For the correlations, to reduce the number of statistical comparisons and focus on the central question of interest—we averaged thresholds over the two smallest gap sizes (0.5 and 1.0 degrees; when the stimulus perceptually approximates a single, large high-contrast stimulus) and the three largest gap sizes (1.5, 2.5, and 4.5 degrees; when the central target stimulus is clearly perceptually isolated). Correlating parietal SA with thresholds revealed no relationship for small gap sizes ($r_{27} = 0.10$, $p = 0.62$) and a significant relationship with large gap sizes ($r_{27} = -0.47$, $p < 0.01$; Figure 6D).

A different, and much simpler, prediction is made for frontal cortex associations with behavior. Revisiting the results of experiment 1 (Figure 4B), larger SA is associated with lower thresholds across all high-contrast stimulus sizes. Similarly, we expect to see an association with frontal cortex SA variation across all stimulus gap sizes in experiment 2. This prediction holds for both the qualitative group split (Figure 6C) and the quantitative analysis of correlations with behavior (Figure 6E). Specifically, correlating frontal SA with thresholds revealed a significant relationship with small ($r_{27} = -0.60$, $p < 10^{-3}$) and large ($r_{27} = -0.37$, $p < 0.05$) gap sizes. Overall, SA variations in frontal and parietal cortices are associated with distinct patterns of behavior that generalize to new stimulus configurations.

Experiment 3: Generalizing the results to a new subject cohort

We examined whether the basic findings could be generalized to a new cohort of participants. For that, we re-analyzed an existing dataset of participants diagnosed with ASD who had previously participated in the motion duration threshold experiment and who also had structural MRIs. These participants ($n = 20$) are a subset of the population we have described in earlier publications; refer Schallmo M.-P et al. and Kolodny T. et al.[23,25] for demographic and clinical characterizations. We found that the summed SA in the same six cortical parcellations (parietal and frontal) was associated with duration thresholds in the average of the two smallest (0.5 and 1.0°), high-contrast conditions (Figure 7; $r_{18} = -0.52$, $p = 0.02$), demonstrating that the cortical SA model extends beyond our experiment 1 and 2 discovery sample. Due to the relatively limited number of participants in the experiment 3 cohort, we did not explore the differential contributions of frontal and parietal cortices.

Experiment 4: The relationship between SA and fMRI responses

Our previous research, along with that of others, has demonstrated a strong connection between neural activity in the hMT+ region and performance in motion duration threshold experiments, supporting a key linking hypothesis between neural responses and behavior. Specifically, greater neural response strength in hMT+ is associated with lower duration thresholds. This relationship has been observed using various techniques such as functional MRI (fMRI),[14,26,27] pharmacology,[28] transcranial magnetic stimulation (TMS),[29] and monkey electrophysiology.[30] In our earlier studies,[22,28] we found that the degree of hMT+ fMRI response to presentations of drifting gratings correlated with duration thresholds measured in psychophysical experiments performed outside the scanner. This finding indicated that individuals with intrinsically stronger hMT+ neural responses tend to have lower duration thresholds.
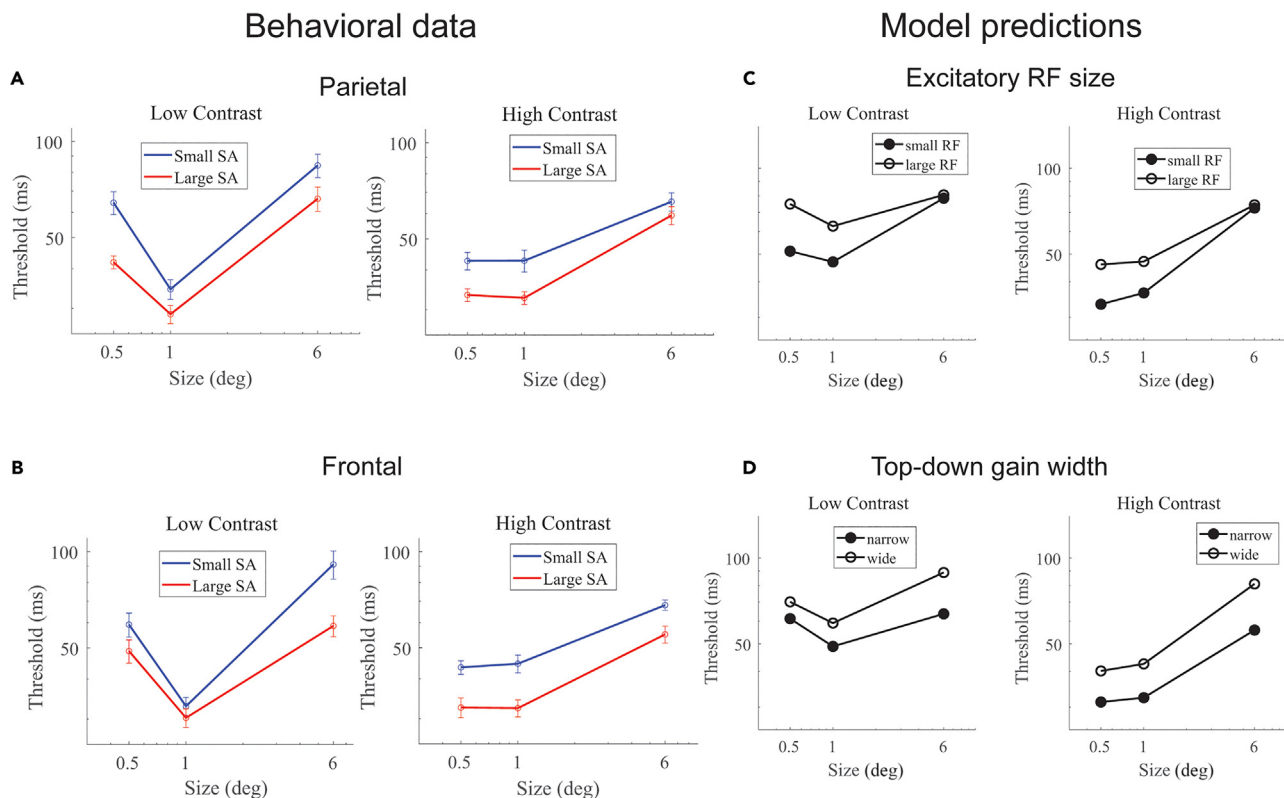
Figure 4. Qualitative analysis

(A and B) Subjects were split into two groups—large and small—based on the size of their parietal region and frontal region SA.

(C and D) Distinct model parameters are associated with the unique behavioral differences across size and contrast. Spatially narrower receptive fields (smaller RFs) produce model predictions that approximate larger parietal SA (A vs. C). Narrower spatial top-down gain produces model predictions that approximate larger frontal SA (B vs. D).

Considering this, we investigated whether cortical SA in the identified parietal or frontal regions was related to fMRI responsiveness in hMT+. Our results showed that individual differences in SA within the frontal region (r_{28} = 0.50, p < 0.01), but not the parietal region (r_{28} = 0.10, p = 0.61), were significantly associated with hMT+ fMRI responsiveness (Figure 8). This further reinforces the idea that the computational architecture in the frontal cortex may contribute to the neural responses underlying task performance.

Experiment 5: Specificity of the findings

It might be the case that variations in frontal and parietal SA could reflect broader cognitive capacities rather than the specific computational roles posited by the divisive normalization model. For example, a larger frontal SA could ostensibly enhance overall task performance, leading to lower motion duration thresholds, thus confounding our interpretation. Our findings presented thus far, however, reveal a more specific effect of SA. For example, the relationship between frontal SA and motion duration thresholds was notably significant only for larger stimulus sizes (6 degrees) under low contrast conditions, as shown in Figure 4B. This specificity in the data challenges the notion that general cognitive performance underlies the observed effects, as such a mechanism would predict a uniform influence across various stimulus sizes and contrasts. Moreover, differential effects observed in the parietal cortex—where significant correlations were observed only under certain conditions (Figure 6B)—further align with predictions from the DN model rather than a generalized cognitive enhancement.

To more directly test the hypothesis that SA impacts are confined to specific visual processing tasks rather than general cognitive performance, we conducted a new experiment focusing on simple contrast detection where performance is not expected to be related to the specific parameters of the model (excitatory RF and attention width). This experiment was designed to assess whether the same regions implicated in motion duration tasks would also influence performance in simple contrast detection. There was no significant association between performance in the contrast detection task and SA in the regions previously linked to motion processing, (frontal: p = 0.60; all parietal: p > 0.14). These findings underscore the specificity of our results to a task with a spatial integration component (motion duration thresholds) and support that the observed relationships between SA and task performance are not the result of general cognitive or perceptual abilities but are likely attributable to the specialized contributions of these regions to visual motion perception as defined by the divisive normalization model.
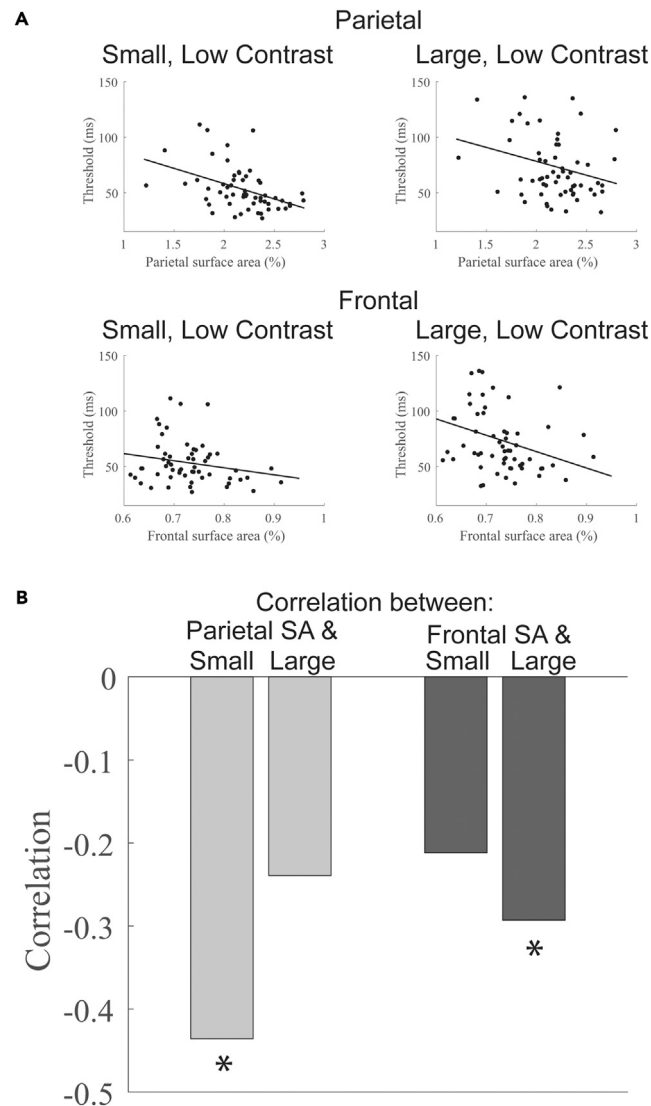
Figure 5. Correlations between motion thresholds for small (0.5 degrees) and large (6.0 degrees) low-contrast stimuli with SA in the parietal and frontal regions

(A) Individual scatterplots.

(B) Correlation values. *p < 0.05.

DISCUSSION

Previous studies have shown substantial individual variation in SA in cortical subregions,[4,5,31] and we hypothesized that this variation may be related to the spatial properties of cortical circuits. We tested this hypothesis by measuring the relationship between SA in cortical subregions and motion duration thresholds. Our results demonstrate that individuals with proportionally larger subregions of parietal and frontal cortices exhibit shorter motion duration thresholds compared to those with smaller regions. Our results suggest unique computational implications of SA in parietal and frontal cortices, with each region associated with different aspects of the normalization model. A cluster of subregions in the right parietal cortex were associated with the spatial extent of excitatory receptive fields; incorporating spatially narrower excitatory receptive fields into the normalization model produced a predicted pattern of thresholds across size and contrast that was similar to that exhibited by individuals with larger SA in these regions. In contrast, a subregion of the left frontal lobe was associated with the width of top-down gain, incorporating spatially narrower top-down gain into the normalization model produced a pattern of predicted thresholds across size and contrast that was similar to individuals with larger SA in this region.

Although we expected *a priori* to find a relationship between parietal cortex SA and thresholds, we did not expect it to be associated with the spatial extent of receptive field size. In fact, our original conceptualization was that the parietal cortex would be associated with the width
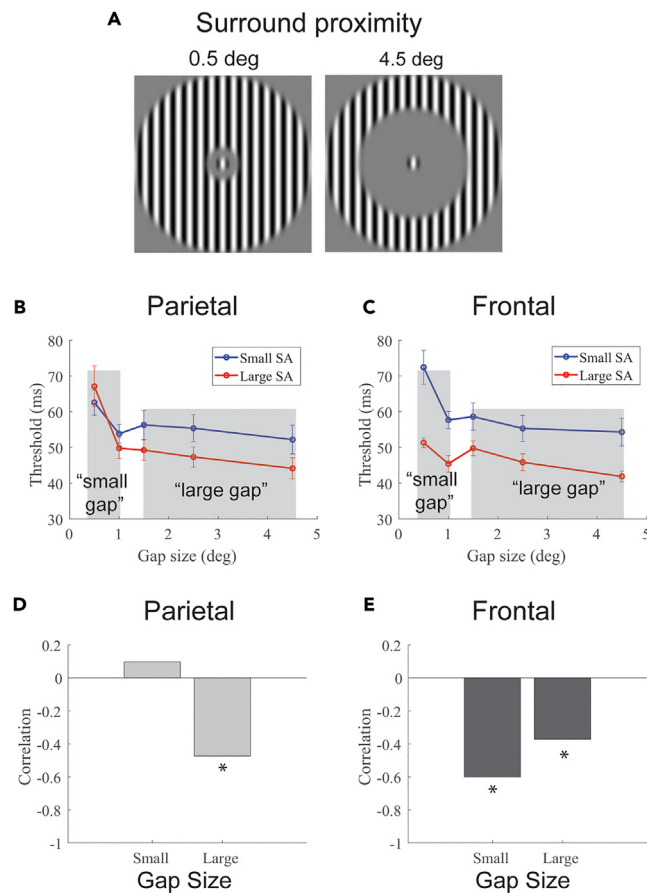
Figure 6. New stimulus configuration

(A) A high-contrast small (0.5 degrees) central target stimulus was used for the motion duration threshold task. An uninformative high-contrast surrounding stimulus could move in either the same or different direction as the central target. The gap size ranged from a minimum of 0.5 deg–4.5 degrees. Subjects were split into two groups based on their SA in parietal (B) and frontal regions.

(C) The nature of the group differences across gap size differed.

(D) Larger parietal SA was associated with lower thresholds only for large gap sizes. *$p < 0.05$.

(E) Larger frontal SA was associated with lower thresholds for all gap sizes. *$p < 0.05$.

of top-down gain, as depicted in Figure 1. The spatial width of excitatory receptive fields would seem to be a property more appropriate for regions directly involved in sensory processing, such as hMT+ or possibly V1. One possibility is that SA is a feature that represents "inherited" properties of its inputs—that the effects of SA on neural computation is more aligned with input than output properties of the region. This possibility is diagrammed in Figure 9 which shows how the excitatory receptive fields of inputs to parietal cortex could be reflected in differences in spatial activation—narrow versus wide for large versus small SA, respectively. In addition, the parietal cortex's unexpected association with the characteristics traditionally attributed to sensory processing regions can also be conceptualized through the lens of "distributed processing." Here, the properties of a region (e.g., SA) might not only reflect its direct computational roles but also its integrative functions within a wider network. This hypothesis is supported by emerging research suggesting that cortical areas, traditionally viewed as dedicated to specific cognitive functions, often participate in multiple overlapping networks that contribute to a variety of tasks. Future work will be required to clarify this level of computational specificity and the degree to which SA is more aligned with spatial properties of inputs, outputs, or some combination of the two.

We did not have strong *a priori* assumptions about the specific contribution of frontal regions. While frontal regions are known to be critical in top-down attentional modulation, the degree to which they are spatiotopically organized is unclear. Thus, in our original hypothesis—depicted in Figure 1—it was unclear whether a region anatomically so far removed from sensory processing would be associated with visual motion processing. However, as the results clearly support—both in the significant relationship with behavior and with the association with fMRI responsiveness in hMT+—subregions of the frontal cortex appear to be strongly associated with visual sensory processing and in a manner consistent with top-down gain within the normalization model. Again, the relationship between SA and circuitry may be more relevant to the input than outputs of the frontal region.
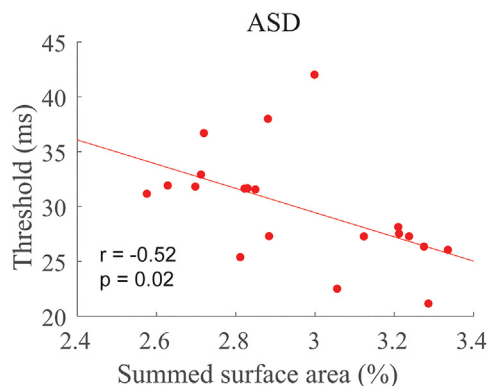
Figure 7. A new cohort
Summed SA across parietal and frontal regions was associated with thresholds in a new cohort of subjects diagnosed with ASD.

While the relationship between visual processing and parietal cortical regions is well-established, featuring clear functional connections to visual processing areas in the occipital-temporal cortex,[32–34] the functional connections of the frontal region (left 11l) we identified are less well-known. However, recent connectomic analyses of the HCP data using the HCP-MMP atlas suggest that region 11l is particularly well-suited to modulate visual responses, either indirectly through strong functional connectivity to IP2 in the parietal lobe (one of the regions where SA correlated with thresholds) or more directly through anatomic connections to V1 via the inferior fronto-occipital fasciculus.[35] In fact, recent findings have suggested that the inferior fronto-occipital fasciculus may play a key a role in tuning early visual processing for efficient task performance.[36]

An additional indication that the association between SA variation and motion duration thresholds is related to spatial attention can be observed in the strong right hemisphere bias of the parietal cortex associations. The right parietal cortex's involvement in spatial attention is well-established across a broad range of methodologies. For example, lesion studies have demonstrated that patients with damage to the right parietal cortex often exhibit spatial neglect, a condition characterized by an inability to attend to or be aware of stimuli in the left side of their visual space.[37,38] This phenomenon is more pronounced and persistent when the lesion occurs in the right hemisphere compared to the left hemisphere.[39] Functional fMRI studies have consistently shown that the right parietal cortex is activated during tasks requiring spatial attention such as orienting, target detection, covert attention shifts, and spatial working memory.[40–43] This asymmetry is further supported by findings that the right parietal cortex exhibits greater functional connectivity with other brain regions involved in attention and perception, such as the frontal eye fields and extrastriate visual cortex.[44,45] Thus, while the motion duration threshold task does not directly manipulate the focus of spatial attention, the fact that individual differences in performance can be well-explained by manipulating the top-down gain parameter of the normalization model and that the relationship between SA variation in parietal cortex and thresholds are strongly right lateralized is consistent with the hypothesis that these associations reflect underlying neural processes related to spatial attention and its modulation by cortical structure.

Interestingly, our findings were not consistent with a simple "more cortex is better" hypothesis. Previous research has shown a positive association between SA in regions traditionally linked to specific behaviors and performance in those behaviors. For example, individuals with larger SA in V1 exhibit lower thresholds in acuity tasks.[4,5,46] Although it is evident that responses in hMT+ are crucial for performance in this task,[14,29,30] we did not observe a relationship between thresholds and SA in visual motion processing regions, such as MT and MST, at least when defined using common atlas-based parcellations. Therefore, while activity in hMT+ may be essential for task performance, it seems that modulation of activity in hMT+ through top-down influences may be critical for determining individual differences in performance.

Our results demonstrate the predictive ability of our findings, as we observed similar associations between cortical SA and duration thresholds in a second task using a new stimulus configuration, as well as in an additional cohort diagnosed with autism spectrum disorder (ASD). This indicates that the relationship between cortical SA and motion duration thresholds extends beyond our initial sample, highlighting the potential of using structural MRI measures to predict task performance in various populations.

Limitations of the study

One potential limitation of our study is the reliance on atlas-based parcellations to define regions of interest. These predefined regions may not fully capture individual variability in the location and size of attentional control and motion processing regions. One possible solution to address this limitation is the use of individualized, targeted functional localizer tasks for defining regions. However, implementing this approach in a large sample would require considerable resources to specify multiple ROIs. An alternative strategy could involve exploring multiple, automatic parcellations to first determine the appropriate spatial scale of SA variation. Although the optimal spatial scale remains unclear, our results were consistent across the regions defined by the HCP-MMP atlas and the visual cortex-optimized Wang (2015) atlas.[47]
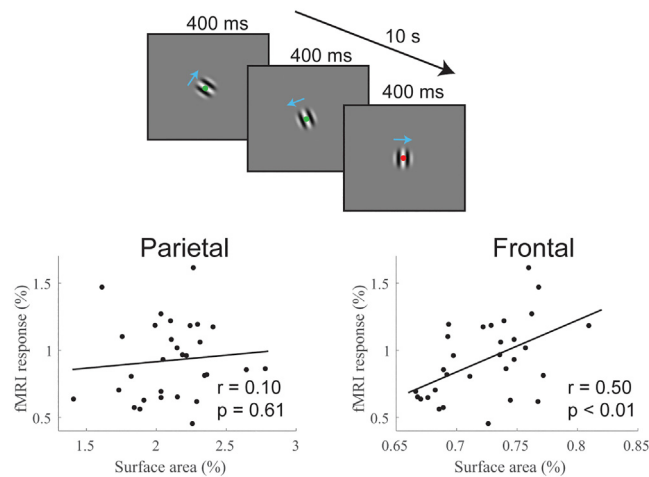
**Figure 8. Association with fMRI responses in hMT+**

Response magnitude in hMT+ was measured in response to briefly presented small, high-contrast gratings. Individual differences in hMT+ responsiveness were associated with SA in frontal but not parietal regions.

Future research should focus on examining SA variation across multiple spatial scales to establish the optimal spatial scale for characterizing SA in the context of brain-behavior associations.

STAR★METHODS

Detailed methods are provided in the online version of this paper and include the following:

- KEY RESOURCES TABLE
- RESOURCE AVAILABILITY
  - Lead contact
  - Materials availability
  - Data and code availability
- EXPERIMENTAL MODEL AND STUDY PARTICIPANT DETAILS
  - Participants
- METHOD DETAILS
  - MRI acquisition
  - Cortical surface area
  - Psychophysics: Visual display and stimuli
  - Psychophysics: Experiment 1 & 3, motion duration thresholds
  - Psychophysics: Experiment 2, motion integration
  - Psychophysics: Experiment 5, contrast detection
  - Functional MRI: Experiment 4, hMT+ responsiveness
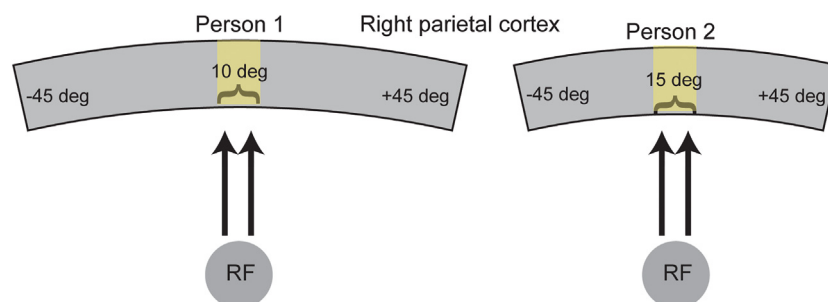
Figure 9. An alternative to the original schematic that highlights the relationship between SA and inputs to a region

Equivalent excitatory inputs would be expected to result in narrow versus wide excitatory drive for large (left) versus small (right) SA.

● QUANTIFICATION AND STATISTICAL ANALYSIS
  ○ Computational model

SUPPLEMENTAL INFORMATION

ACKNOWLEDGMENTS

AUTHOR CONTRIBUTIONS

S.O.M. conceived the study. S.O.M. and T.K. performed data analyses. S.O.M., T.K., and S.J.W. interpreted the results and wrote the manuscript.

DECLARATION OF INTERESTS

The authors declare no competing interests.

REFERENCES

1. Vuoksimaa, E., Panizzon, M.S., Chen, C.-H., Fiecas, M., Eyler, L.T., Fennema-Notestine, C., Hagler, D.J., Jr., Franz, C.E., Jak, A.J., Lyons, M.J., et al. (2016). Is bigger always better? The importance of cortical configuration with respect to cognitive ability. Neuroimage *129*, 356–366.

2. Zacharopoulos, G., Klingberg, T., and Kadosh, R.C. (2020). Cortical surface area of the left frontal pole is associated with visuospatial working memory capacity. Neuropsychologia *143*, 107486.

3. Vuoksimaa, E., Panizzon, M.S., Chen, C.-H., Fiecas, M., Eyler, L.T., Fennema-Notestine, C., Hagler, D.J., Fischl, B., Franz, C.E., Jak, A., et al. (2015). The genetic association between neocortical volume and general cognitive ability is driven by global surface area rather than thickness. Cereb. Cortex *25*, 2127–2137.

4. Song, C., Schwarzkopf, D.S., Kanai, R., and Rees, G. (2015). Neural population tuning links visual cortical anatomy to human visual perception. Neuron *85*, 641–656.

5. Duncan, R.O., and Boynton, G.M. (2003). Cortical magnification within human primary visual cortex correlates with acuity thresholds. Neuron *38*, 659–671.

6. Rimol, L.M., Nesvåg, R., Hagler Jr, D.J., Bergmann, Ø., Fennema-Notestine, C., Hartberg, C.B., Haukvik, U.K., Lange, E., Pung, C.J., Server, A., et al. (2012). Cortical volume, surface area, and thickness in schizophrenia and bipolar disorder. Biol. Psychiatry *71*, 552–560.

7. Bois, C., Ronan, L., Levita, L., Whalley, H.C., Giles, S., McIntosh, A.M., Fletcher, P.C., Owens, D.C., Johnstone, E.C., and Lawrie, S.M. (2015). Cortical surface area differentiates familial high risk individuals who go on to develop schizophrenia. Biol. Psychiatry *78*, 413–420.

8. Cheng, W., Frei, O., van der Meer, D., Wang, Y., O'Connell, K.S., Chu, Y., Bahrami, S., Shadrin, A.A., Alnæs, D., Hindley, G.F., et al. (2021). Genetic association between schizophrenia and cortical brain surface area and thickness. JAMA Psychiatr. *78*, 1020–1030.

9. Palaniyappan, L., Mallikarjun, P., Joseph, V., White, T.P., and Liddle, P.F. (2011). Regional contraction of brain surface area involves three large-scale networks in schizophrenia. Schizophr. Res. *129*, 163–168.

10. Hazlett, H.C., Poe, M.D., Gerig, G., Styner, M., Chappell, C., Smith, R.G., Vachet, C., and Piven, J. (2011). Early brain overgrowth in autism associated with an increase in cortical surface area before age 2 years. Arch. Gen. Psychiatry *68*, 467–476.

11. Mensen, V.T., Wierenga, L.M., van Dijk, S., Rijks, Y., Oranje, B., Mandl, R.C., and Durston, S. (2017). Development of cortical thickness and surface area in autism spectrum disorder. Neuroimage. Clin. *13*, 215–222.

12. Ecker, C., Ginestet, C., Feng, Y., Johnston, P., Lombardo, M.V., Lai, M.-C., Suckling, J., Palaniyappan, L., Daly, E., Murphy, C.M., et al. (2013). Brain surface anatomy in adults with autism: the relationship between surface area, cortical thickness, and autistic symptoms. JAMA Psychiatr. *70*, 59–70.

13. Tadin, D., Lappin, J.S., Gilroy, L.A., and Blake, R. (2003). Perceptual consequences of centre–surround antagonism in visual motion processing. Nature *424*, 312–315.

14. Schallmo, M.-P., Kale, A.M., Millin, R., Flevaris, A.V., Brkanac, Z., Edden, R.A., Bernier, R.A., and Murray, S. (2018). Suppression and facilitation of human neural responses. Elife *7*, e30334.

15. Reynolds, J.H., and Heeger, D.J. (2009). The normalization model of attention. Neuron *61*, 168–185. https://doi.org/10.1016/j.neuron.2009.01.002.

16. Carandini, M., and Heeger, D.J. (2011). Normalization as a canonical neural computation. Nat. Rev. Neurosci. *13*, 51–62.

17. Silver, M.A., Ress, D., and Heeger, D.J. (2005). Topographic maps of visual spatial attention in human parietal cortex. J. Neurophysiol. *94*, 1358–1371.

18. Sereno, M., Pitzalis, S., and Martinez, A. (2001). Mapping of contralateral space in retinotopic coordinates by a parietal cortical area in humans. Science *294*, 1350–1354.

19. Silver, M.A., and Kastner, S. (2009). Topographic maps in human frontal and parietal cortex. Trends Cogn. Sci. *13*, 488–495.

20. Saygin, A.P., and Sereno, M.I. (2008). Retinotopy and attention in human occipital, temporal, parietal, and frontal cortex. Cereb. Cortex *18*, 2158–2168.

21. Foss-Feig, J.H., Tadin, D., Schauder, K.B., and Cascio, C.J. (2013). A substantial and unexpected enhancement of motion perception in autism. J. Neurosci. *33*, 8243–8249. https://doi.org/10.1523/JNEUROSCI.1608-12.2013.

22. Murray, S.O., Schallmo, M.-P., Kolodny, T., Millin, R., Kale, A., Thomas, P., Rammsayer, T.H., Troche, S.J., Bernier, R.A., and Tadin, D. (2018). Sex differences in visual motion processing. Curr. Biol. *28*, 2794–2799.e3.

23. Schallmo, M.-P., Kolodny, T., Kale, A.M., Millin, R., Flevaris, A.V., Edden, R.A., Gerdts, J., Bernier, R.A., and Murray, S.O. (2020). Weaker neural suppression in autism. Nat. Commun. *11*, 2675.

24. Glasser, M.F., Coalson, T.S., Robinson, E.C., Hacker, C.D., Harwell, J., Yacoub, E., Ugurbil, K., Andersson, J., Beckmann, C.F., Jenkinson, M., et al. (2016). A multi-modal parcellation of human cerebral cortex. Nature *536*, 171–178.

25. Kolodny, T., Schallmo, M.P., Gerdts, J., Edden, R.A., Bernier, R.A., and Murray, S.O. (2020). Concentrations of Cortical GABA and Glutamate in Young Adults With Autism Spectrum Disorder. Autism Res. *13*, 1111–1129.

26. Turkozer, H.B., Pamir, Z., and Boyaci, H. (2016). Contrast affects fMRI activity in middle temporal cortex related to center–surround interaction in motion perception. Front. Psychol. 7, 454.

27. Er, G., Pamir, Z., and Boyaci, H. (2020). Distinct patterns of surround modulation in V1 and hMT. Neuroimage 220, 117084.

28. Schallmo, M.-P., Millin, R., Kale, A.M., Kolodny, T., Edden, R.A., Bernier, R.A., and Murray, S.O. (2019). Glutamatergic facilitation of neural responses in MT enhances motion perception in humans. Neuroimage 184, 925–931.

29. Tadin, D., Silvanto, J., Pascual-Leone, A., and Battelli, L. (2011). Improved motion perception and impaired spatial suppression following disruption of cortical area MT/V5. J. Neurosci. 31, 1279–1283.

30. Liu, L.D., Haefner, R.M., and Pack, C.C. (2016). A neural basis for the spatial suppression of visual motion perception. Elife 5, e16167.

31. Benson, N.C., Yoon, J.M., Forenzo, D., Engel, S.A., Kay, K.N., and Winawer, J. (2022). Variability of the surface area of the V1, V2, and V3 maps in a large sample of human observers. J. Neurosci. 42, 8629–8646.

32. Kay, K.N., and Yeatman, J.D. (2017). Bottom-up and top-down computations in word-and face-selective cortex. Elife 6, e22341.

33. Saalmann, Y.B., Pigarev, I.N., and Vidyasagar, T.R. (2007). Neural mechanisms of visual attention: how top-down feedback highlights relevant locations. Science 316, 1612–1615.

34. Takemura, H., Rokem, A., Winawer, J., Yeatman, J.D., Wandell, B.A., and Pestilli, F. (2016). A major human white matter pathway between dorsal and ventral visual cortex. Cereb. Cortex 26, 2205–2214.

35. Baker, C.M., Burks, J.D., Briggs, R.G., Stafford, J., Conner, A.K., Glenn, C.A., Sali, G., McCoy, T.M., Battiste, J.D., O'Donoghue, D.L., and Sughrue, M.E. (2018). A Connectomic Atlas of the Human Cerebrum—Chapter 4: The Medial Frontal Lobe, Anterior Cingulate Gyrus, and Orbitofrontal Cortex. Oper. Neurosurg. 15, S122–S174.

36. Uithol, S., Bryant, K.L., Toni, I., and Mars, R.B. (2021). The anticipatory and task-driven nature of visual perception. Cereb. Cortex 31, 5354–5362.

37. Bisiach, E. (1988). Hemineglect in humans. Handb. Neuropsychol. 1, 195–222.

38. Heilman, K.M., Valenstein, E., and Watson, R.T. (1984). Neglect and related disorders. Seminars in neurology, Vol. 4 (Thieme Medical Publishers, Inc.), pp. 209–219.

39. Morrow, L.A., and Ratcliff, G. (1988). The disengagement of covert attention and the neglect syndrome. Psychobiology 16, 261–269.

40. Corbetta, M., Kincade, J.M., Ollinger, J.M., McAvoy, M.P., and Shulman, G.L. (2000). Voluntary orienting is dissociated from target detection in human posterior parietal cortex. Nat. Neurosci. 3, 292–297.

41. Postle, B., Awh, E., Jonides, J., Smith, E., and D'Esposito, M. (2004). The where and how of attention-based rehearsal in spatial working memory. Brain Res. Cogn. Brain Res. 20, 194–205.

42. Silk, T.J., Bellgrove, M.A., Wrafter, P., Mattingley, J.B., and Cunnington, R. (2010). Spatial working memory and spatial attention rely on common neural processes in the intraparietal sulcus. Neuroimage 53, 718–724.

43. Zuanazzi, A., and Cattaneo, L. (2017). The right hemisphere is independent from the left hemisphere in allocating visuospatial attention. Neuropsychologia 102, 197–205.

44. Vincent, J.L., Kahn, I., Snyder, A.Z., Raichle, M.E., and Buckner, R.L. (2008). Evidence for a frontoparietal control system revealed by intrinsic functional connectivity. J. Neurophysiol. 100, 3328–3342.

45. Heinen, K., Feredoes, E., Ruff, C.C., and Driver, J. (2017). Functional connectivity between prefrontal and parietal cortex drives visuo-spatial attention shifts. Neuropsychologia 99, 81–91.

46. Himmelberg, M.M., Winawer, J., and Carrasco, M. (2022). Linking individual differences in human primary visual cortex to contrast sensitivity around the visual field. Nat. Commun. 13, 3309.

47. Wang, L., Mruczek, R.E., Arcaro, M.J., and Kastner, S. (2015). Probabilistic maps of visual topography in human cortex. Cereb. Cortex 25, 3911–3931.

48. Kolodny, T., Schallmo, M.-P., Gerdts, J., Bernier, R.A., and Murray, S.O. (2020). Response dissociation in hierarchical cortical circuits: a unique feature of autism spectrum disorder. J. Neurosci. 40, 2269–2281.

49. Mowinckel, A.M., and Vidal-Piñeiro, D. (2020). Visualization of brain statistics with R packages ggseg and ggseg3d. Advances in Methods and Practices in Psychological Science 3, 466–483.

50. Brainard, D.H., and Vision, S. (1997). The psychophysics toolbox. Spat. Vis. 10, 433–436.

51. Pelli, D.G., and Vision, S. (1997). The VideoToolbox software for visual psychophysics: Transforming numbers into movies. Spat. Vis. 10, 437–442.

52. Kleiner, M., Brainard, D., and Pelli, D. (2007). What's new in Psychtoolbox-3? Perception 36, 1–16.

53. Kingdom, F.A.A., and Prins, N. (2016). Psychophysics: A Practical Introduction, 2nd edition (London: Academic Press).

54. Power, J.D., Barnes, K.A., Snyder, A.Z., Schlaggar, B.L., and Petersen, S.E. (2012). Spurious but systematic correlations in functional connectivity MRI networks arise from subject motion. Neuroimage 59, 2142–2154.

55. Siegel, J.S., Power, J.D., Dubis, J.W., Vogel, A.C., Church, J.A., Schlaggar, B.L., and Petersen, S.E. (2014). Statistical improvements in functional magnetic resonance imaging analyses produced by censoring high-motion data points. Hum. Brain Mapp. 35, 1981–1996.

STAR★METHODS

KEY RESOURCES TABLE

REAGENT or RESOURCE	SOURCE	IDENTIFIER
Software and algorithms		
Matlab 2022b	https://www.mathworks.com/products/matlab.html	RRID:SCR_001622
R Project for Statistical Computing	http://www.r-project.org/	RRID:SCR_001905
Python Programming Language	http://www.python.org/	RRID:SCR_008394
FreeSurfer (7.2.0)	http://surfer.nmr.mgh.harvard.edu/	RRID:SCR_001847

RESOURCE AVAILABILITY

Lead contact

Further information and request for resources should be directed to and will be fulfilled by the lead contact, Scott Murray (somurray@uw.edu).

Materials availability

This study did not generate new unique reagents.

Data and code availability

- Data reported in this paper will be shared by the lead contact upon request.
- No unique code was generated, but analysis code is available from the lead contact upon request.
- Any additional information required to reanalyze the data reported in this paper is available from the lead contact upon request.

EXPERIMENTAL MODEL AND STUDY PARTICIPANT DETAILS

Participants

The inclusion criteria for participants in all experiments were as follows: age 18-30 years, non-verbal IQ >70, normal or corrected to normal visual acuity, no visual impairments, no impairment to sensory or motor functioning, no history of seizures or diagnosis of epilepsy, and no neurological disease or history of serious head injury. A total of 73 participants participated in Experiment 1, with a subset of 30 of these participants described in previous publications.[14,22] Due to poor psychophysical data quality, 11 participants were excluded from the analysis as their staircases failed to estimate a reliable threshold. These participants were identified and removed through a combination of an automatic algorithm (described in the psychophysics section below) and visual inspection. Consequently, the results of a total of 62 participants are reported in Experiment 1. For five participants, thresholds for the smallest (0.5 deg) condition were not measured, so when reporting statistical analyses that include this condition, 57 participants are included. All other analyses include the full set of 62 participants. Experiment 2 (alternative stimulus configuration) included 32 participants from the original 73 participants who participated in Experiment 1. The psychophysical data from three of these participants were excluded from analysis due to poor psychophysical data quality. A summary of participant demographics for each Experiment is provided in Table 1. All procedures were approved by the University of Washington Institutional Review Board (STUDY #: 00000556) and all participants provided written informed consent. The race and ethnicity of the participants reflected the composition of the University of Washington community and was approximately 70 percent White, 4 percent Black, 18 percent Asian, and 7 percent Hispanic.

The participants in experiment 3 were individuals with ASD, who were included in previous publications.[23,25,48] Full diagnostic characterization can be found in these previous reports. A total of 23 autistic individuals had complete data across the necessary stimulus conditions, and three were removed using the same data quality exclusion procedures, resulting in a total of 20 subjects.

A portion of the fMRI data in experiment 4 have been included in previous publications[22,28,48] and represent a subset of the subjects that also had psychophysical data (n = 30).

METHOD DETAILS

MRI acquisition

MRI data of experiments 3 & 4 were acquired using a Philips 3-Tesla Achieva scanner. MRI data of the remaining 43 participants in experiment 1 (including the participants of experiment 2) were acquired using a Philips 3-Tesla Ingenia Elition scanner. In both scanners, a 32-channel high-resolution head coil was used. High resolution T1-weighted anatomical images were acquired for each participant using a magnetization prepared rapid acquisition gradient echo (MPRAGE) protocol (TR = ~7.7 msec, TE = ~3.5 msec, flip angle = 7°, 176 1 mm thick slices, 256 × 256 × 176 matrix, voxel resolution: 1 × 1 × 1 mm). There were no differences in SA between participants scanned in the different scanners.

Cortical surface area

Cortical surface area was measured using FreeSurfer (7.2.0). The HCP-MMP atlas was projected onto the cortical surface of each subject using FreeSurfer's mri_surf2surf command and the lh/rh.HCP-MMP1.annot annotation file. Statistics, including surface area (mm), were generated using FreeSurfer's mris_anatomical_stats command. Unless noted, all surface area values were normalized to the total cortical surface area per hemisphere (for example, RH_V1_normalized = (RH_V1/(sum(all_RH_parcels))) * 100). With 180 parcels per hemisphere, each region comprised roughly 0.5 to 1.5% of the total hemispheric cortical surface area. To extract surface area for the Wang et al. (2015) atlas, the Python library Neuropythy was used with its "atlas" function. Once applied, the Python Nibabel library was used to extract surface area values. These values were normalized using the total cortical surface per hemisphere derived from the FreeSurfer atlas. Visualization (Figure 3) was done using the R package ggseg.[49]

Grouping subjects based on large and small total cortical SA was achieved by first calculating the sum of normalized SA in the parietal/frontal cortex regions that correlated with duration thresholds. Next, the top 1/3 and bottom 1/3 of subjects in total SA were selected to form the groups (Figures 4A and 4B). For experiment 2 (Figures 6B and 6C), groups were created using the top and bottom halves of subjects, due to the smaller overall number of participants.

Psychophysics: Visual display and stimuli

Our experimental apparatuses and stimuli have been described in our recent publications.[14,23] We used a ViewSonic PF790 CRT monitor (120 Hz) and Bits# stimulus processor (Cambridge Research Systems, Kent, UK). Stimuli were created and displayed in MATLAB (MathWorks, Natick, MA) and PsychToolbox.[50–52] Viewing distance for all experiments was 66 cm, and luminance was linearized using a PR650 spectrophotometer (Photo Research, Chatsworth, CA). Stimuli were sinusoidally modulated luminance gratings presented on a mean luminance background. Vertically oriented gratings drifted either left or right (drift rate = 4 cycles/s) within a circular aperture, which was blurred with a Gaussian envelope (SD = 0.21°). We used three different stimulus sizes: 0.5°, 1.5°, and 6° in diameter. The Michelson contrast of the gratings was either 3% (low) or 98% (high), and the spatial frequency was 1.2 cycles/°.

Psychophysics: Experiment 1 & 3, motion duration thresholds

Participants discriminated the direction of motion (left or right) of a briefly presented drifting grating. Trials began with a shrinking circle fixation mark (850 ms) at the center of the screen, followed by a vertical grating, and then a response period (no time limit). Grating duration was adjusted across trials (range 6.7–333 ms) according to an adaptive (Psi) staircase procedure implemented within the Palamedes toolbox.[53] Correct responses tended to yield shorter durations on subsequent trials, adjusting the grating duration to find the briefest presentation for which the participant would perform with 80% accuracy. Each staircase consisted of 25 trials. Six independent staircases (3 sizes × 2 contrasts) were included in each run and were randomly interleaved across trials. A total of four runs were included in each experimental session, which began with examples and practice runs to familiarize subjects with the procedure. Total task duration was approximately 30 minutes.

Duration thresholds for motion direction discrimination were calculated by fitting a Weibull function to the data from each individual staircase. Guess rate and lapse rate were fixed at 50% and 4%, respectively. Thresholds were calculated from the fit psychometric function as the duration value where the participant performed with 80% accuracy. The median of the four threshold estimates was used as the final threshold estimate for a particular condition.

Because individual differences in thresholds are central to the analyses, extra care was taken to ensure accurate threshold estimates for each subject. Staircase quality was determined by calculating the ratio of the threshold estimates across trials. The average estimate of the final 5 trials of the staircase was divided by the average estimate of the first 10 trials. If this ratio exceeded 0.8, the staircase was removed from the average. This procedure detects "rising staircases" near the end of the trial sequence and was confirmed via visual inspection to identify unreliable estimates. A subject with 4 or more flagged staircases was considered for exclusion. For excluded subjects, the algorithm identified, on average, 5 staircases per subject for removal. For included subjects, the algorithm identified, on average, 1 staircase per subject. However, the algorithm sometimes failed to detect staircases when errors occurred near the beginning of the trial sequence; these errors result in particularly high threshold estimates at the beginning of the sequence. These cases were determined through visual inspection (See Data S6 for examples of different data quality situations).

Psychophysics: Experiment 2, motion integration

Experiment 2 was the same as Experiment 1 in all respects except that it used a single, small (0.5 deg) target grating and a surrounding grating that could move in either the same or opposite direction as the target. The gap size between the outer edge of the target and the inner edge of the surround varied, including 0.5, 1.0, 1.5, 2.5, and 4.5 degrees. The widest portion of the surrounding grating extended to 7.75 degrees. Trials were also included that had no surround. One staircase per stimulus condition was included in each of four runs, and staircases were interleaved across trials. Each staircase was composed of 25 trials. In this report, only data from the 5 gap sizes for the same-direction surround are presented.

Psychophysics: Experiment 5, contrast detection

For contrast detection, the task was to detect whether a grating (sinusoidal luminance modulation within a Gaussian window, SD = 0.42°, FWHM = 1°, 1.5 cycles/°, vertical or horizontal orientation) was presented at the center of a mean gray background during either the first

or second of two possible stimulus presentation intervals. Stimulus contrast was adjusted using the same Psi staircase procedure as the motion duration experiments to determine the lowest contrast that could be detected with 80% accuracy (i.e., the threshold). Full description of the methodological details can be found in.[22]

Functional MRI: Experiment 4, hMT+ responsiveness

Portions of the fMRI data have been described previously[22,28,48] and are a subset of the sample in Experiment 1. Briefly, the fMRI measurements were designed to assess individual differences in responsiveness in hMT+ to stimuli that approximated the stimuli used in the psychophysical experiment. As such, a block-design was used that varied stimulus contrast across blocks (3%) and (98%). The scans began with a blank block in which only the fixation mark was presented on a mean gray background. Blocks of drifting gratings (2° diameter) were then presented centrally in an alternating order, each followed by a blank block, to permit the fMRI response to return to baseline (6 low-contrast blocks, 6 high contrast, and 13 blank per run). During a stimulus block, drifting gratings of different direction were presented for 400 ms. Subjects each completed 2–4 runs of the contrast experiment. Throughout all blocks in all functional scans, participants were engaged in a conjunctive color-shape detection task in the center of the screen, to encourage fixation and maintain engagement and wakefulness. Participants were instructed to press a button when a green circle appeared in a series of small, briefly presented color shapes.

Functional localizer scans were acquired to identify the hMT+ regions-of-interest (ROI). To identify human MT complex (hMT+) stimuli were sinusoidal luminance modulated gratings at 15% contrast. Stimuli were the same size and had the same spatial frequency as the experimental stimuli, and were presented in the same retinotopic locations, without edge blurring. Blocks of drifting gratings (4 cycle/°, same drift rate of the experimental stimuli) alternated with blocks of static gratings, each block 10 s long, for a total of 24 blocks per scan.

Data were preprocessed using BrainVoyager QX v2.8.4 (Brain Innovation) software. EPI data were motion-corrected, corrected for distortion due to magnetic field inhomogeneities, high-pass filtered, and coregistered to the AC–PC aligned T1 structural scan. ROIs were identified from the localizer scan data using correlational analyses with an initial threshold of $p < 0.05$ (Bonferroni corrected). ROIs were defined for each hemisphere in the anatomical region of motion-selective MT in the lateral occipital lobe. Average time courses across the 20 most significantly active (from the localizer scan) voxels in each ROI were determined for each block. Percentage-transformed time courses were then calculated for each block: first, for each stimulus block, we extracted 12 time points corresponding to -4 s before stimulus onset to 18 s after stimulus onset. Then we converted the values to percentage signal change relative to the mean value of the three time points before stimulus onset. To extract a univariate measure to be used in the statistical analyses, the average response magnitude in time points 8–12 s was calculated from each of these time courses. Some blocks/runs were excluded from averaging because of head motion or low task performance, according to the following criteria: data for a given block was excluded because of head motion if the framewise displacement in successive TRs was >0.9 mm,[54,55] up to and including 8 TRs before the stimulus block or 2 TRs after it. If more than one-half the blocks of either condition were excluded, or a subject had a hit rate of <60% in the central fixation task, the whole run was excluded.

QUANTIFICATION AND STATISTICAL ANALYSIS

Computational model

The normalization model used in this study is the same as in recent publications[14,23] and is based on the instantiation first described by Reynolds and Heeger.[15] The model is useful for making qualitative comparisons between versions using different parameters. It is employed to make predictions in the motion duration threshold task by assuming that thresholds are inversely proportional to response magnitude – a higher neural response in the model results in a lower predicted duration threshold. The scalar value used as the model response is the maximum value of the population response image. A scaling factor, applied across all stimulus conditions, is used to convert the model response to milliseconds. The comparison of differences in the width of top-down gain used the same model as reported previously to account for differences between autistic and non-autistic subjects in this same motion duration threshold task.[23] The version used to characterize differences in the spatial width of excitatory drive held all other parameters constant and used values of 3 and 4.5 for the excitatory drive widths (arbitrary units). The version used to characterize differences in the attention width used values of 3 and 7 (arbitrary units). MATLAB code is available upon request that implements these models. Since the primary hypothesis is that cortical surface area affects spatial circuitry, we also explored the only other spatial characteristic of the model: the spatial pooling width of the divisive normalization. This did not yield predictions that were related to the observed pattern of behavior as a function of SA differences, only serving to additively shift predicted thresholds.